Hindawi Publishing Corporation
Journal of Nanomaterials
Volume 2015, Article ID 692648, 7 pages
http://dx.doi.org/10.1155/2015/692648

Research Article

Understanding the High Ionic Conductivity in Nanostructured Ytterbium Stabilized Zirconia Thin Films

A. Benítez-Rico,[1] M. F. García-Sánchez,[2] M. Picquart,[3] B. M. Monroy-Peláez,[1] and G. Santana-Rodríguez[1]

[1]*Instituto de Investigaciones en Materiales, Universidad Nacional Autónoma de México, Ciudad Universitaria, Circuito Exterior s/n, A.P. 70-360, Coyoacán, 04510 México, DF, Mexico*
[2]*Unidad Profesional Interdisciplinaria en Ingeniería y Tecnologías Avanzadas, Instituto Politécnico Nacional, Avenida I.P.N. 2580, Gustavo A. Madero, 07340 México, DF, Mexico*
[3]*Departamento de Física, Universidad Autónoma Metropolitana, A.P. 55-534, Iztapalapa, 09340 México, DF, Mexico*

Correspondence should be addressed to G. Santana-Rodríguez; gsantana1963@yahoo.com.mx

Received 27 February 2015; Accepted 28 July 2015

Academic Editor: Weihua Shen

Copyright © 2015 A. Benítez-Rico et al. This is an open access article distributed under the Creative Commons Attribution License, which permits unrestricted use, distribution, and reproduction in any medium, provided the original work is properly cited.

Recently, high ionic conduction has been reported in nanostructured materials. This increase in conductivity can be important in technological applications, including micro-Solid Oxide Fuel Cells, so the understanding of this phenomenon is essential. In this work, XRD, Raman spectroscopy, SEM, EDS maps, and UV-Visible spectroscopy measurements are used to have an insight into the relationship between structural and electrical properties in nanostructured ytterbium stabilized zirconia (YbSZ) thin films prepared by ultrasonic spray pyrolysis. Raman measurements allowed the identification of a mixture of tetragonal and cubic phases at 4% of Yb doping, which cannot be detected by XRD, while the compositional maps suggest that Yb can be located preferentially in the grain boundaries. Changes in the activation energy values in bulk and grain boundaries are related to the small grain sizes (≤10 nm). UV measurements support the ionic nature of the charge transport. These results indicate that the high conductivity is a consequence of different physical parameters in the films such as stress in the materials, different crystalline phases, impurities diffusion to the grain boundaries, and the presence or absence of electronic conduction. A model that explains the increase of conductivity in nanostructured materials must include all these aspects.

1. Introduction

The search for clean and renewable energy sources is imperative today. Solid Oxide Fuel Cell (SOFC) technology has a substantial potential for application in clean and efficient electric power generation. A SOFC is an electrochemical conversion device that produces electricity directly from oxidizing hydrogen (a zero-emission fuel) at temperatures that can be as high as 1000°C. This high temperature is essentially due to the low ionic conductivity of solid electrolytes at lower temperatures. There is significant interest in decreasing the SOFC operating temperature to an intermediate range to improve chemical and mechanical stability and reduce the cost, increasing its competitiveness [1]. Enhancing the ionic transport in the electrolyte and cathode materials is a key factor for this purpose. Recently, it has been demonstrated that nanostructured materials and nanoscale heterolayered oxides show increased transport properties, which reinforces their potential as electrolytes in SOFC [2–6]. But the physical basis of this phenomenon is not fully understood yet [7–11].

Yttrium stabilized zirconia (YSZ) has long been used as electrolyte in Solid Oxide Fuel Cells. The specific grain boundary conductivity in polycrystalline electrolytes is usually at least two orders of magnitude lower than that of the grain bulk, leading to a blocking effect of oxygen ion transport as well as lower ionic conductivities at low temperatures. In order to improve the conductivity in grain boundaries, the optimization of synthesis processes for such materials is of great importance. During the last years, considerable attention has been focused on the deposition of smooth, homogeneous, and dense nanostructured thin films of YSZ for μ-SOFC applications [1–3, 12–14]. However, it is known

that there are other rare earth dopants that can be used to stabilize zirconia with better electrical performance, in particular, Yb [15]. A lot of previous works have been devoted to studying the properties of bulk ytterbia stabilized zirconia [16–18]; however nanostructured thin films of this material have been little explored as electrolyte for applications in μ-SOFC.

Among the varieties of deposition processes available to prepare ytterbium stabilized zirconia (YbSZ) thin films, the spray pyrolysis techniques are very attractive for industrial applications since they allow the deposition of a wide variety of ceramic films over large areas with a simple process at low costs. In particular, ultrasonic spray deposition (USD) can generate a small and homogeneous droplet size which results in high quality films. Among other benefits, it also offers the possibility to dope thin films just by adding a salt containing the dopant atom to the spray solution precursor. This technique was originally used for production of nanometer-sized powders [20]. However, it can also be optimized to obtain thin films with nanometric grain size [3, 4].

In a previous work, we prepared nanostructured YbSZ thin films with high ionic conduction [5]. Since grain boundaries are the limiting factor in the conductivity of polycrystalline materials and nanostructured materials increase considerably the amount of grain boundaries, this is a contradictory result without explanation. While transport mechanisms in bulk materials are well understood, interfacial transport mechanisms in these materials are still a promising research field. In order to contribute to the understanding of the physical basis behind the increased ionic conductivity in these nanomaterials, in this work we focus on the morphology, compositional homogeneity, and optical band gap of nanostructured YbSZ thin films in order to gain insights to explain the unique electrical properties of these materials.

2. Materials and Methods

The experimental setup shown in García-Sánchez et al. [3] was used. Both (100) n-type, 200 Ω·cm single crystalline silicon slices and Corning glass were used as substrates. The precursor solution was prepared by dissolving calculated mixtures of zirconium (IV) acetylacetonate (98%) and ytterbium acetate tetrahydrate (99.9%) from Sigma-Aldrich Chemicals in anhydrous methanol (Fisher 99.9%). Different ytterbium/zirconium molar ratios (between 0.04 and 0.12 mol percent) were used, the substrate temperature was fixed at 550°C, and the carrier and director gas flow rates were 1.5 L/min and 3.5 L/min, respectively. More details were reported in [5]. Thermal annealing at 700°C was performed to all the samples in order to improve the crystallinity and avoid the presence of organic residues from precursors.

Surface morphology and energy dispersive X-ray analyses were performed with a field-emission scanning electron microscope JEOL-7600F at 1 kV and 15 kV, respectively. The samples were observed in planar view without any further preparation, using low voltages to avoid surface charging. X-ray diffraction patterns were obtained with a Rigaku DMAX 2200 equipment using the CuKα wavelength, the XRD spectra were obtained for theta angles from 2° to 70° with steps of 0.020°. The unit cell parameters were calculated using the Celref3 program.

The Raman spectra were recorded using a T64000 Jobin-Yvon Horiba triple monochromator using a microscope objective ×100. The excitation source was the 514.5 nm line from an Ar+ Lexcel laser. All measurements were performed at room temperature in open air. The sample was irradiated at a power of 20 mW at the laser head. Ten accumulations with an integration time of 1 min were performed on each sample in the range 10–1200 cm^{-1}. The Raman signal was detected by a cooled CCD. Transmittance measurements were recorded in a UV-Vis spectrometer Jasco V-630 in a two-beam configuration. The optical band gap was calculated by the Tauc model from the UV-Vis transmission data.

AC conductivity was measured using a frequency-response analyzer (SOLARTRON SI 1260 with dielectric interface) in the frequency range 0.01 Hz–10 MHz to investigate the electrical properties for temperatures between 100 and 450°C. A parallel pattern of two platinum electrodes was sputtered on the film surface to be used as electrodes. Impedance diagrams were simulated, using the Zview program, by a series network of two subcircuits, each one consisting of one resistor and one Constant Phase Element (CPE) in parallel, as detailed in our previous work [5].

3. Results and Discussion

Figure 1 presents the XRD pattern for the film grown with 4% of ytterbium. In the same figure the theoretical peaks corresponding to tetragonal (JCPDS file number 017-0923) and cubic (JCPDS file number 013-0307) zirconia phases are presented [5]. It is noteworthy that the XRD signals corresponding to these two phases are overlapped. Three crystalline phases are reported in stabilized zirconia: monoclinic, tetragonal, and cubic. The cubic phase is the most stable one and it is usually assumed to be present in the XRD pattern. But other phases have been reported in nanometric zirconia thin films or for low dopant concentrations [15, 19–22]. The solid solution is substitutional where the Yb^{3+} ions occupy the Zr^{4+} ion sites, creating oxygen vacancies (inset of Figure 1). The presence of different crystalline structures is associated with the differences in cation sizes, along with the possible ordering of Yb^{3+} ions and, consequently, the oxygen vacancies. As the ionic conduction depends directly on the vacancies distribution, precise phase identification is important to analyze the conduction mechanisms in these materials. But this precise phase identification is very difficult by XRD.

Raman measurements were performed in order to clarify the identity of the crystalline phases in these films (Figure 2). The Raman spectra of oxide ceramics typically contain a large amount of information, extracted from the band positions, their intensities, and their shapes. The spectra of the tetragonal, cubic, and monoclinic phases of zirconia are sufficiently different to enable a qualitative analysis [23]. Each structure exhibits specific features that can be assigned to an actual spectral signature of the studied phases. In Table 1 we show all the peaks reported for the different

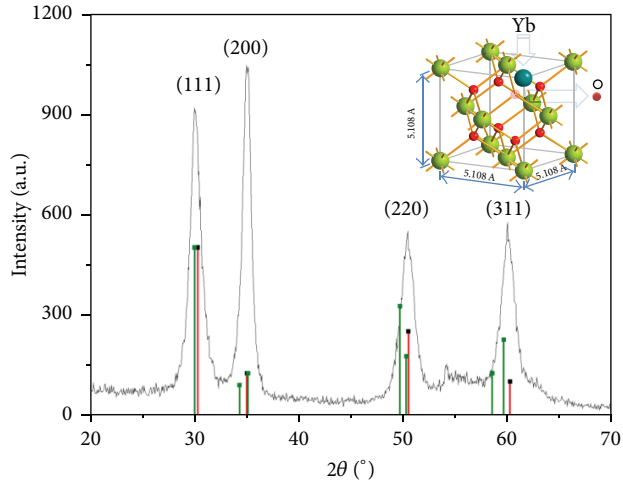

Figure 1: XRD pattern of the film grown with 4% of ytterbium. The theoretical reflections of the cubic (red) and tetragonal (green) phases in YbSZ are presented in the figure. The crystalline structure where the Yb positions and vacancies are presented is shown in the inset. Reprinted with permission from [5].

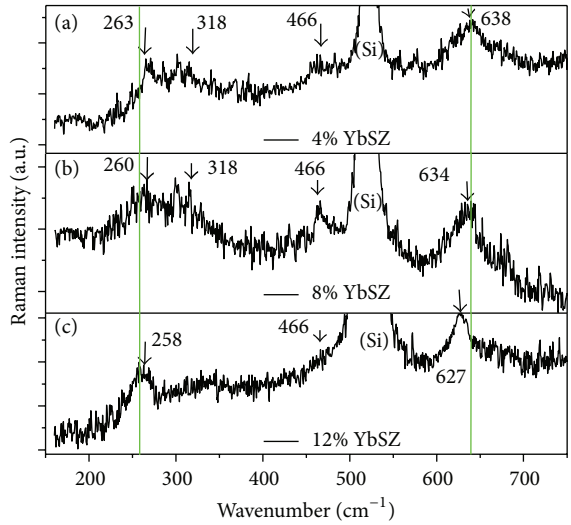

Figure 2: Raman spectra of samples with 4, 8, and 12% of ytterbium.

phases of zirconia. For the monoclinic phase, 13 peaks are distinguished, notably a doublet at 178 and 190 cm^{-1} and an intense peak at 474 cm^{-1}, which are not appreciated in the spectra of Figure 2. Nevertheless, small peaks around 303 cm^{-1} are present for low Yb concentrations, indicating that traces of monoclinic phase can be present in the samples, as noted before in XRD measurements [5]. On the other hand, for the tetragonal phase, five peaks are distinguished. The most characteristic are a sharp band at 142 cm^{-1}, a broader band from 250 cm^{-1} to 350 cm^{-1}, and two other peaks localized at 466 and 638 cm^{-1}. The first peak does not appear in the Raman spectra of Figure 2, but the last two peaks are clearly observed for low Yb concentrations

Table 1: Reported peaks for different zirconia phases (cm^{-1}) [19].

Cubic	Tetragonal	Monoclinic
142	**142**	
		178
		190
		219
256	**256**	
		303
	320	331
		345
		379
466	**466**	
		474
		500
		534
		559
		615
628	**637**	638

(Figure 2(a and b)), which indicates the presence of the tetragonal phase. The similarities between the spectra corresponding to cubic and tetragonal phases are explained by the proximity in their crystal lattice parameters. In Table 1 we underline the coincident peaks between tetragonal and cubic phases in bold font. The most representative difference between Figure 2(a, b and c) is the shift observed in the position of the band at 627 cm^{-1} corresponding to the oxygen and cation ions F_{2g} stretching Raman mode of the cubic phase with respect to the position of the band at 638 cm^{-1} corresponding to the tetragonal phase. This indicates that for the samples presented in Figure 2(a and b) mixtures of tetragonal and cubic phases are present. As the ytterbium percent in the zirconia matrix increases, the peak tends towards 627 cm^{-1} demonstrating that with increasing Yb concentrations our samples are stabilized in the cubic phase.

The presence of stress in the network can cause shifts of the Raman frequencies. Therefore, the observed Raman shifts corresponding to the different bands shown in Figure 2(a and b) can be induced by the residual stress caused by the change in network parameters between cubic and tetragonal phases. The largest shifts are observed at lower Yb impurity concentrations due to the mixture of phases existing in these materials while a minor shift in the peaks is observed for the samples stabilized in the cubic phase as shown in Figure 2(c). But the latter can only be analyzed from a qualitative point of view because it is very difficult to quantify how stressed the films are based on the observed shifts due to multiple factors involved during Raman measurements.

XRD and Raman results evidenced a mixture of phases at low concentrations of ytterbium in the films. In order to relate these results with the electrical properties, the lattice parameter, grain size, activation energy, and total conductivity at 450°C reported in our previous work [5] are presented

Table 2: Structural and electrical properties of prepared films. Reprinted with permission from [5].

Yb (%)	Grain size (nm)	Lattice parameter (nm)	E_a (eV)* (grains)	E_a (eV)* (grain boundaries)	σ_{total}* $(\Omega cm)^{-1}$
4	6.6	5.10 ± 0.03	0.55	0.89	0.64
6	9.7	5.09 ± 0.02	0.68	0.47	0.32
8	5.3	5.10 ± 0.03	0.82	0.29	0.17
10	10.6	5.10 ± 0.02	0.87	0.47	0.054
12	6.9	5.11 ± 0.02	1.40	0.29	0.021

* E_a represents the activation energy and σ_{total} the total conductivity at 450°C.

in Table 2. With grain sizes between 5.3 and 10.6 nm and a lattice parameter of 0.51 nm, around 28 to 55% of the unit cells in the grain are located in the surface. Then, stress in the lattice, inferred from the Raman spectra, is a very important factor. However, the link between grain size, lattice-strain state, and ionic transport remains unclear. The presence of stress in the grains influences two important conduction processes: the migration space, quantified as the cation-cation distance that represents a bottleneck for the oxygen migration, and the bond strength between the oxygen and the nearest cation preventing the oxygen from migrating. Recent theoretical studies indicate that the macroscopic oxygen diffusivity increases exponentially in YSZ up to a critical value of biaxial tensile strain, with a more significant impact at lower temperatures [8]. In strained regions, the cationic or anionic lattice positions can be off-centred compared to the zero-strained bulk ceramics. Moreover, the electrical conductivity of polycrystalline thin films is influenced by the intrinsic space charge effect and extrinsic segregation of impurities to the grain boundaries [24]. Keppner et al. [11] developed a model where they can estimate the thickness of the strained interface due to mismatch between YSZ/Y_2O_3 thin films. The interface thickness, which determines the point at which the initial strain is relaxed to a value $1/e$, is between 8 and 11 nm. Even when taking into account the differences in preparation, we note that the reported interface thicknesses are in the order of the grain sizes reported in this work.

The maximum conductivity is obtained for films with 4% of Yb (Table 2), which contrasts with the results in bulk materials where the maximum of conductivity is reported at 8–10% of Yb. Moreover, the activation energy of grains increases with the ytterbium percent, while the activation energy of grain boundaries decreases [5]. Even when the presence of stress partially explains the conductivity in grains, other morphological and compositional aspects must be considered. Figure 3 shows SEM images of films with 4, 8, and 12% of ytterbium precursor. The figure shows that the morphology presents important changes with the Yb compositions at the nanometric scale. Films with 4% of Yb are dense and smooth, although some nanocracks are observed in the surface. When the Yb composition increases to 8%, a rougher surface is observed. For compositions higher than 12%, the amount and size of cracks increase. It is important to mention that the cracks cannot be observed at lower resolutions. As all samples were measured in the same conditions and the cracks are specifically located in between grains, we speculate that these changes in morphology are related to differences in the grain boundaries, in the intergrain connection, and maybe in the composition.

Figure 4 shows a compositional map of Yb, Zr, and O in the film with 4% of Yb. A homogeneous distribution of O and Zr in the film can be observed (Figures 4(a) and 4(c)). In contrast, the ytterbium distribution shows black holes (Figure 4(b)). This distribution can be due to the fact that there is only 4% of Yb in the film. On the other hand, it could also be related with a preferential location of Yb in the grain boundaries. Even though EDS analysis is not conclusive, Yb migration to the grain boundaries has an important effect in the electrical properties as discussed in the following part. Research about elements diffusion (Si, Fe) has demonstrated that grain boundary diffusion of cations is commonly many orders of magnitude faster than bulk diffusion in metal oxides with fluorite structure [24]. The increment in conductivity and the decrease in activation energy for grain boundaries can be explained in the context of the space charge effect theory. The space charge potential can be changed by the doping or in-diffusion of aliovalent ions along the grain boundary. For example, effective negative charges can be introduced into the grain boundaries through substitution of Zr^{4+} by Yb^{3+}, resulting in a decrease of the space charge potential. Meng et al. [24] reported an increase of 6-7 times in conductivity for YSZ columnar films after Fe diffusion into the grain boundaries. It is not possible to quantify the elemental composition in grain boundaries by EDS, but it can be a very important aspect that affects the reported increase in conductivity. There are other aspects which must be considered in the understanding of high ionic conduction in grain boundaries. If a percent of the grain boundaries block totally the ionic conduction, increasing the amount of grain boundaries also increases the percolative ways of conduction, which can be another cause for the high ionic conduction in nanocrystalline materials.

In some cases, the increase in conductivity is associated with the presence of electronic conduction in the material. Figure 5 presents the absorption coefficient for the sample with 4% of ytterbium deposited onto a Corning glass substrate. It is the sample with higher conductivity. The obtained optical gap is too high (3.7 eV) compared to the conduction activation energy reported in Table 2 [5]. This indicates that

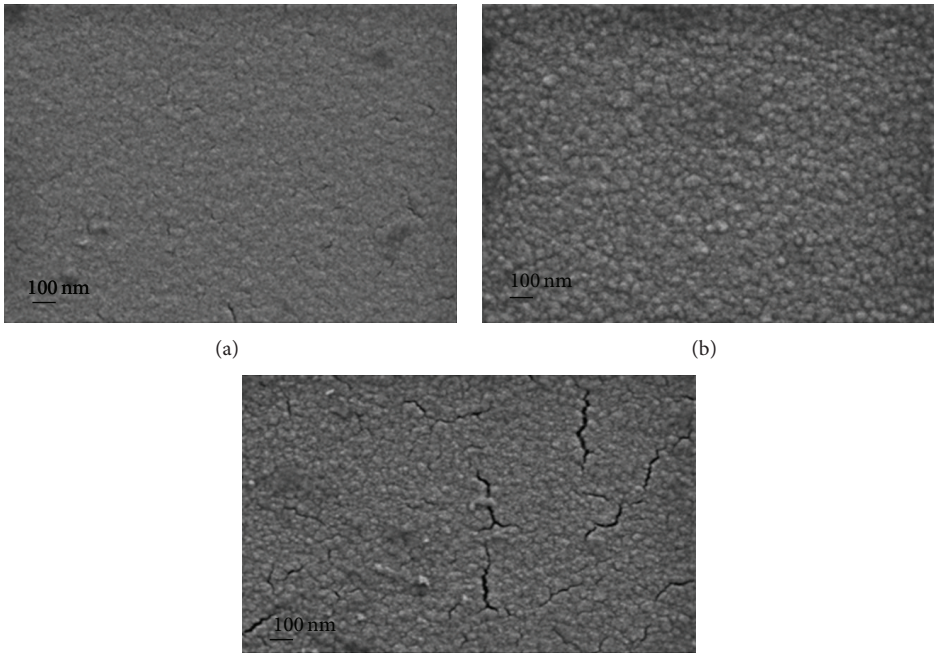

(a) (b)

(c)

Figure 3: SEM images of films with 4 (a), 8 (b), and 12% (c) of ytterbium.

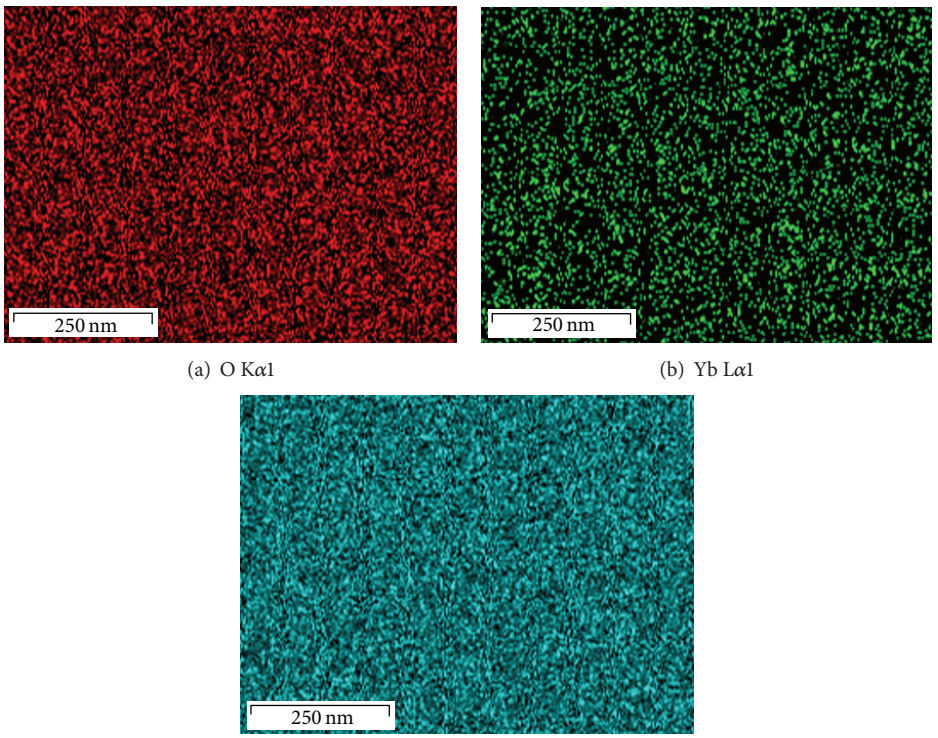

(a) O Kα1 (b) Yb Lα1

(c) Zr Lα1

Figure 4: EDS map of (a) oxygen, (b) ytterbium, and (c) zirconium.

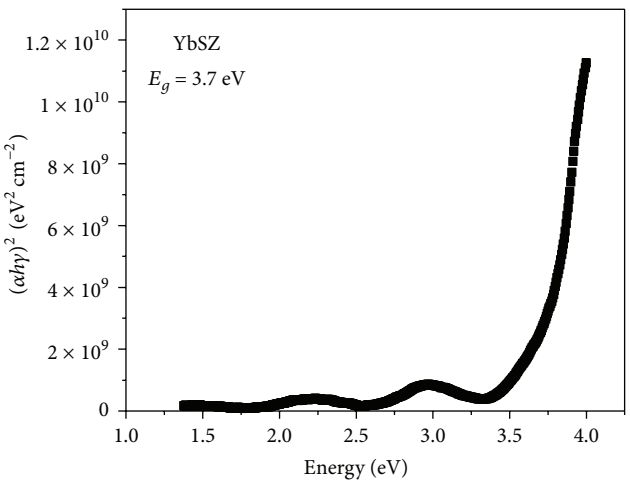

Figure 5: Absorption coefficient spectra for sample with 4% of ytterbium.

the electronic conduction should not be representative in the conductivity values reported in Table 2.

4. Conclusions

In this work, Raman spectroscopy measurements allowed the identification of a mixture of zirconia tetragonal and cubic phases with 4–8% of Yb, which cannot be detected by XRD. Compositional maps suggest that Yb can be located preferentially in the grain boundaries, which can decrease the space charge potential in these regions and be one of the causes of the anomalous increase of grain boundary conductivities. Changes in the activation energy values in grain and grain boundaries are related to the small grain sizes. The fact of obtaining the maximum conductivity at 4% of ytterbium (which is lower than the one reported in bulk materials) may be related with the stress and the mixture of phases (cubic and tetragonal). However, the changes in morphology and composition have a very important influence, especially in the analysis of the grain boundaries conduction, which determines the total conduction in these materials. UV measurements show that the films have a wide electronic band gap, higher than 3.5 eV in all samples. On the other side, the conductivity activation energy is lower than 1 eV, which indicates the ionic nature of the charge transport.

These results indicate that the high conductivity in nanostructured ionic conductors is a consequence of different physical parameters in the films. Therefore, the stress in the materials, different crystalline phases, impurities diffusion to the grain boundaries, and the presence of electronic conduction can all affect the electric properties of nanostructured thin films. They are not independent variables, as the stress induces changes in the crystalline phase and can modify the electronic conduction or favours the impurities diffusion. A model that explains the increase of conductivity in nanostructured materials must include all these aspects. Divergences in the published results can be related to the fact that all these parameters change with the deposition technique, the analyzed material, and the sintering conditions.

Conflict of Interests

The authors declare that there is no conflict of interests regarding the publication of this paper.

Acknowledgments

The authors acknowledge the technical assistance of J. E. Romero-Ibarra, C. Flores, O. Novelo, and M. E. Villafuerte's Laboratory of IIM-UNAM, A. Esparza of CCADET-UNAM, and P. Altuzar of IER-UNAM. The authors acknowledge financial support for this work from CONACYT-SENER under Contract No. 151076 and PAPIIT-UNAM projects IN108215 and IN100914. This work was partially supported from IPN with research Project 20140321 and CONACyT, Mexico, under Projects 153948 and 179632. The author Benítez-Rico wishes to acknowledge the financial support provided by the Grant CONACyT CVU/177386.

References

[1] Z. Shao, W. Zhou, and Z. Zhu, "Advanced synthesis of materials for intermediate-temperature solid oxide fuel cells," *Progress in Materials Science*, vol. 57, no. 4, pp. 804–874, 2012.

[2] I. Kosacki, C. M. Rouleau, P. F. Becher, J. Bentley, and D. H. Lowndes, "Nanoscale effects on the ionic conductivity in highly textured YSZ thin films," *Solid State Ionics*, vol. 176, no. 13-14, pp. 1319–1326, 2005.

[3] M. F. García-Sánchez, J. Peña, A. Ortiz et al., "Nanostructured YSZ thin films for solid oxide fuel cells deposited by ultrasonic spray pyrolysis," *Solid State Ionics*, vol. 179, no. 7-8, pp. 243–249, 2008.

[4] M. F. García-Sánchez, A. Ortiz, G. Santana et al., "Synthesis and characterization of nanostructured cerium dioxide thin films deposited by ultrasonic spray pyrolysis," *Journal of the American Ceramic Society*, vol. 93, no. 1, pp. 155–160, 2010.

[5] A. Benitez-Rico, M. F. García-Sánchez, B. M. Monroy-Pelaez, J. Santoyo-Salazar, M. López-López, and G. Santana-Rodriguez, "High ionic conduction in nanocrystalline ytterbium stabilized zirconia grown by ultrasonic spray pyrolysis," *International Journal of Engineering Science and Innovative Technology*, vol. 3, no. 3, pp. 156–165, 2014.

[6] J. Garcia-Barriocanal, A. Rivera-Calzada, M. Varela et al., "Colossal ionic conductivity at interfaces of epitaxial ZrO_2:Y_2O_3/$SrTiO_3$ heterostructures," *Science*, vol. 321, no. 5889, pp. 676–680, 2008.

[7] X. Guo, "Can we achieve significantly higher ionic conductivity in nanostructured zirconia?" *Scripta Materialia*, vol. 65, no. 2, pp. 96–101, 2011.

[8] A. Kushima and B. Yildiz, "Oxygen ion diffusivity in strained yttria stabilized zirconia: where is the fastest strain?" *Journal of Materials Chemistry*, vol. 20, no. 23, pp. 4809–4819, 2010.

[9] J. L. M. Rupp, "Ionic diffusion as a matter of lattice-strain for electroceramic thin films," *Solid State Ionics*, vol. 207, pp. 1–13, 2012.

[10] W. Shen, J. Jiang, C. Ni, Z. Voras, T. P. Beebe Jr., and J. L. Hertz, "Two-dimensional vacancy trapping in yttria doped ceria," *Solid State Ionics*, vol. 255, pp. 13–20, 2014.

[11] J. Keppner, C. Korte, J. Schubert, W. Zander, M. Ziegner, and D. Stolten, "XRD analysis of strain states in epitaxial YSZ/RE_2O_3

(RE = Y, Er) multilayers as a function of layer thickness," *Solid State Ionics*, vol. 273, pp. 2–7, 2015.

[12] M. V. F. Schlupp, B. Scherrer, H. Ma et al., "Influence of microstructure on the cross-plane oxygen ion conductivity of yttria stabilized zirconia thin films," *Physica Status Solidi A: Applications and Materials Science*, vol. 209, no. 8, pp. 1414–1422, 2012.

[13] D. Beckel, A. Bieberle-Hütter, A. Harvey et al., "Thin films for micro solid oxide fuel cells," *Journal of Power Sources*, vol. 173, no. 1, pp. 325–345, 2007.

[14] A. Evans, A. Bieberle-Hütter, J. L. M. Rupp, and L. J. Gauckler, "Review on microfabricated micro-solid oxide fuel cell membranes," *Journal of Power Sources*, vol. 194, no. 1, pp. 119–129, 2009.

[15] P. S. Patil, "Versatility of chemical spray pyrolysis technique," *Materials Chemistry and Physics*, vol. 59, no. 3, pp. 185–198, 1999.

[16] T. Pramananda Perumala, V. Sridharb, K. P. N. Murthyb, K. S. Easwarakumarc, and S. Ramasamy, "Molecular dynamics simulations of oxygen ion diffusion and superionic conduction in ytterbia-stabilized zirconia," *Computational Materials Science*, vol. 38, no. 4, pp. 865–872, 2007.

[17] J. Feng, X. Ren, X. Wang, R. Zhou, and W. Pan, "Thermal conductivity of ytterbia-stabilized zirconia," *Scripta Materialia*, vol. 66, no. 1, pp. 41–44, 2012.

[18] O. Yamamoto, "Solid oxide fuel cells: fundamental aspects and prospects," *Electrochimica Acta*, vol. 45, no. 15-16, pp. 2423–2435, 2000.

[19] M. Jouanne, J. F. Morhange, M. A. Kanehisa et al., "Structural transformations in nanosized zirconium oxide," *Physical Review B*, vol. 64, no. 15, Article ID 155404, 2001.

[20] B. S. Vasile, O. R. Vasile, C. Ghitulica et al., "Yttria totally stabilized zirconia nanoparticles obtained through the pyrosol method," *Physica Status Solidi (A)*, vol. 207, no. 11, pp. 2499–2504, 2010.

[21] M. Hartmanova, F. Kubel, V. Buršíková et al., "Phase composition-dependent physical and mechanical properties of $Yb_xZr_{1-x}O_{2-x/2}$ solid solutions," *Journal of Physics and Chemistry of Solids*, vol. 69, no. 4, pp. 805–814, 2008.

[22] V. Barbashov, E. Nesova, N. Pismenova, and O. Radionova, "Evidence of induced structural and conduction anisotropy in scandia-stabilized zirconia ceramics," *Physica Status Solidi A: Applications and Materials Science*, vol. 209, no. 4, pp. 727–729, 2012.

[23] G. Pezzotti, K. Yamada, S. Sakakura, and R. P. Pitto, "Raman spectroscopic analysis of advanced ceramic composite for hip prosthesis," *Journal of the American Ceramic Society*, vol. 91, no. 4, pp. 1199–1206, 2008.

[24] B. Meng, M. Kong, Q. Q. Yang, H. Zhang, Y. J. Zhu, and Z. L. Lin, "Effects of grain-boundary diffusions and modifications on the electrical conductivities of YSZ coatings with columnar microstructure," *Solid State Ionics*, vol. 268, pp. 48–53, 2014.

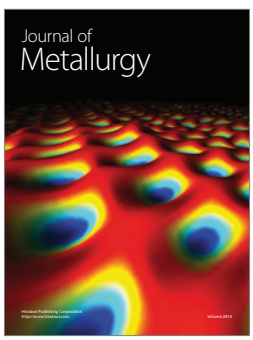

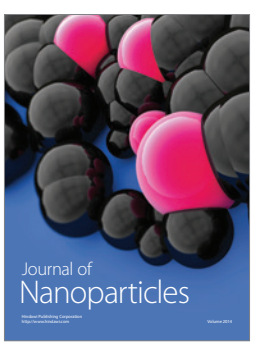

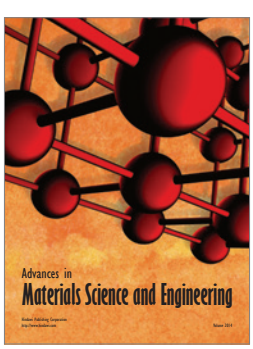

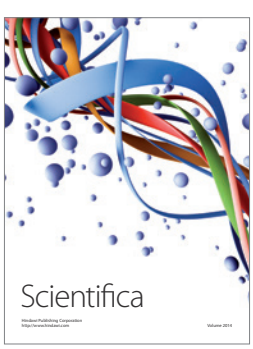

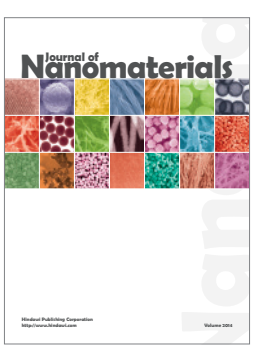

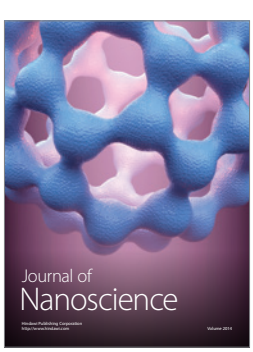

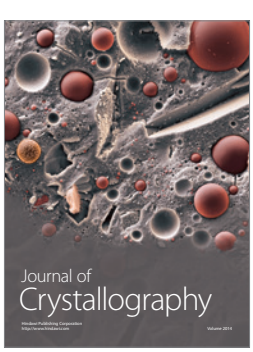

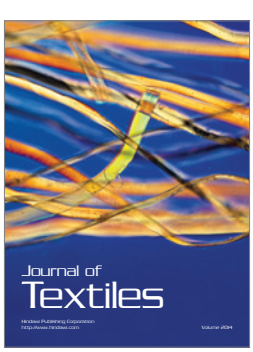

Hindawi

Submit your manuscripts at
http://www.hindawi.com